Malekan, Mohammad; Khosravi, Ali; St-Pierre, Luc

An Abaqus plug-in to simulate fatigue crack growth

Published in:
Engineering with Computers

DOI:
10.1007/s00366-021-01321-x

Published: 18/02/2021

Document Version
Peer-reviewed accepted author manuscript, also known as Final accepted manuscript or Post-print

Published under the following license:
Unspecified

Please cite the original version:
Malekan, M., Khosravi, A., & St-Pierre, L. (2021). An Abaqus plug-in to simulate fatigue crack growth. *Engineering with Computers*. https://doi.org/10.1007/s00366-021-01321-x

An Abaqus plug-in to simulate fatigue crack growth

Mohammad Malekan[1], Ali Khosravi[2], Luc St-Pierre[2]

[1] Department of Mechanical and Production Engineering, Aarhus University, 8000 Aarhus C, Denmark
[2] Department of Mechanical Engineering, Aalto University, Espoo, Finland

Abstract

Fatigue crack propagation is an important consideration in evaluating the design life of engineering components, especially in the energy and transport industries. Despite its importance, fatigue analyses are not usually supported by commercial Finite Element (FE) codes; in fact, most FE codes require the addition of costly plug-ins to perform fatigue crack growth simulations. Therefore, this paper introduces a new, freely-distributed plug-in to simulate fatigue crack growth with the commercial FE code Abaqus. The plug-in includes five different fatigue crack growth models and relies on the extended FE method to simulate crack propagation. The plug-in is limited to 2D analyses, but covers all necessary steps for fatigue crack growth simulations; from creating the geometry to job submission and post-processing. The implementation of the plug-in is validated by comparing its predictions to analytical and experimental results. Finally, we hope that the simplicity of the plug-in and the fact that it is distributed freely will make it a useful simulation tool for industrial, research and educational purposes.

Keywords: *Fatigue crack growth; Abaqus plug-in; Python scripting; Finite element method; Life estimation*

Nomenclature

a	crack length (mm)
Δa	crack growth incremental length (mm)
A	material constant
A_k, B_k	fitting constants
C, m	Paris law empirical coefficients
C_n, n, p, q	NASGRO empirical coefficients
C_f, m_f	Forman law empirical coefficients
C_w, m_w	Walker law empirical coefficients
da/dN	crack growth rate in length/cycle
E	Young's modulus (GPa)
Γ	contour integral
G	energy release rate
I	Interaction energy integral
J	J-integral
K_I, K_{II}	mode-I and mode-II stress intensity factors ($\mathrm{MPa}\sqrt{\mathrm{m}}$)
K_C	fracture toughness ($\mathrm{MPa}\sqrt{\mathrm{m}}$)
K_{IC}	mode-I fracture toughness ($\mathrm{MPa}\sqrt{\mathrm{m}}$)
K_{crit}	critical value of SIF ($\mathrm{MPa}\sqrt{\mathrm{m}}$)
K_{max}, K_{min}	SIF for the maximum and minimum loads in the cycle ($\mathrm{MPa}\sqrt{\mathrm{m}}$)
ΔK	SIF range ($\mathrm{MPa}\sqrt{\mathrm{m}}$)
ΔK_{eq}	equivalent ΔK for mixed-mode loading condition ($\mathrm{MPa}\sqrt{\mathrm{m}}$)
ΔK_{th}	threshold ΔK ($\mathrm{MPa}\sqrt{\mathrm{m}}$)
ΔK_w	Walker ΔK ($\mathrm{MPa}\sqrt{\mathrm{m}}$)
γ	material constant
N	number of cycles
N_i	number of cycles at each iteration
P	applied load (N)
P_{max}	maximum applied load (N)
p_e, q_e	material constants
R	stress ratio
r	point distance from crack-tip point
S_{max}, S_{min}	maximum and minimum stresses (MPa)
σ_{yld}	yield strength (MPa)
σ_{ij}, ϵ_{ij}	stress and strain tensors
t	thickness (mm)
t_0	reference thickness related to the state of plane strain
θ_c	crack front kinking angle (deg)
W	width of the specimen (mm)
W_{enrg}	strain energy density

Abbreviations

CT	compact tension
CCT	center-cracked specimen in tension
DCT	disk-shaped CT specimen
FCG	fatigue crack growth
FE	finite element
FEM	FE method
LEFM	linear elastic fracture mechanics
SIF	stress intensity factor
SEB	single-edge bending specimen
SEN	single-edge notched specimen
SENT	single-edge notched under tension
XFEM	extended FEM

1 Introduction

Fatigue is responsible of most mechanical failures in the machinery, transport and maritime industries [1, 2, 3]. Many studies have been focused on fatigue mechanisms and crack growth models since the mid-20th century, proposing different fatigue propagation laws and analyses of different phenomena such as crack closure [4, 5, 6, 7, 8, 9]. Since fatigue tests are long and expensive, engineers are increasingly relying on numerical predictions to prevent fatigue failures [10, 11]. Even though the Finite Element (FE) method is routinely employed in structural design, most commercial FE codes do not support directly fatigue analysis. Therefore, additional plug-ins or toolkits are necessary to perform fatigue predictions. These fatigue analyses can be divided in two main categories:

1. Fatigue life. Here, the component studied is pristine (no cracks), and fatigue failure is predicted based on Stress-cycle (SN) curves, or similar approaches based on cyclic strains. Plug-ins and toolkits, such as FPU [12] and FE Safe, already exist for this type of analysis, which is not the main focus of this paper.
2. Fatigue crack growth predictions. In this case, the part includes one or multiple cracks and the simulations aim to predict both the crack growth per cycle, and the direction of crack propagation. This category is the main focus of the paper.

Plug-ins and toolkits have been developed to simulate fatigue crack propagation, and these are listed in Table 1 along with their main characteristics. All tools listed in Table 1 are designed for the commercial FE software Abaqus, with the exception of Zencrack which can also interface with Ansys and NX Nastran. They are all capable of performing 3D analyses, but they employ different approaches to model crack propagation. The FCG-system represents the crack explicitly in the part's geometry, whereas Zencrack uses specific crack blocks elements. More recent approaches, such as XFA3D and Morfeo/crack, rely on the extended Finite Element Method (XFEM) to model crack growth. This technique is more computationally efficient since crack growth can be simulated without remeshing.

The tools listed in Table 1 suffer from an important limitation: none of them are distributed freely. This can be problematic particularly in research and education, where the number of simulations is often too small to justify the purchase of a new software. This is the main reason why we have developed a new plug-in to simulate fatigue crack propagation.

The plug-in introduced in this paper is also designed for the commercial FE software Abaqus, and relies on XFEM to simulate crack propagation. The plug-in is limited to 2D analyses, but it offers several advantages. First, it offers a variety of options to model crack growth: the plug-in has five approaches to compute the stress intensify factor range for mixed-mode loading, and it includes five different fatigue crack growth laws (more than some of the tools presented in Table 1). Second, the plug-in is easy to use since all inputs are entered through a single Graphical User Interface (GUI). Third, the tool covers all aspects of fatigue crack growth analysis; from defining the geometry and material properties, running the analysis, and visualizing the results. With all these advantages, we believe the plug-in can be an extremely useful tool to simulate fatigue crack propagation, especially for research and educational purposes.

The paper is structured as follows. First, an overview of the plug-in is presented. Second, all inputs necessary for the plug-in are reviewed in details. Finally, the implementation of the plug-in is validated by comparing its predictions to analytical and experimental results taken from the literature.

Table 1. Comparison of tools to simulate fatigue crack propagation.

Plug-in/Toolkit	Works with	2D/3D	Crack modeling	Freely distributed
Zencrack [13]	Abaqus/Ansys/NX Nastran	3D	Crack blocks	no
XFA3D [14]	Abaqus	3D	XFEM	no
Morfeo/Crack [15]	Abaqus	3D	XFEM	no
FCG-System [16]	Abaqus	3D shell elements	Explicitly in part geometry	no
Fatlab [17]	Ansys	2D/3D	No	yes

This plug-in[1] [18]	Abaqus	2D	XFEM	yes

2 Structure of the plug-in

This section begins with an overview of the plug-in, followed by more specific details on each part of the plug-in. This Abaqus plug-in covers all stages from pre- to post-processing: it can automatically create the FE model, run the fatigue crack growth analysis, and plot the results requested. The modelling approach followed by the plug-in is described in Figure 1 with a flowchart. It includes four main steps:

1. A FE model of the component is created with the boundary conditions and loads representative of a single fatigue cycle. The plug-in allows the user to import their own geometry or use one of six standard specimens (see Section 2.1). Currently, the plug-in is limited to 2D plane stress or plane strain analyses, and to linear elastic material properties. The plug-in relies on the extended finite element method (XFEM) to model crack propagation. This technique allows the user to specify the location of the initial crack simply with coordinates rather than explicitly modeling the flaw in the part geometry.

2. Abaqus performs a linear elastic calculation (a static, general step in Abaqus notation) and extract how the stress intensity factors K_I and K_{II} vary during a single loading cycle. Abaqus also computes the angle of crack propagation θ_c, which is illustrated in Figure 2. There are three different approaches to calculate θ_c, but they are all depend on K_I and K_{II}.

3. The plug-in computes all fatigue crack growth parameters. Using K_I and K_{II} obtained in Step 2, the plug-in first calculates the stress intensity factor range ΔK_i. The plug-in offers five different approaches to compute ΔK_i, all of them taken from the literature. Then, the plug-in computes the number of cycles ΔN_i required to grow the crack by Δa, which is a user input. This is done using one of the five fatigue crack growth laws implemented in the plug-in. All laws express the fatigue crack growth rate $\mathrm{d}a/\mathrm{d}N$ as a function of ΔK, and therefore if the crack growth increment Δa is small we can estimate the number of cycles ΔN_i with:

$$\frac{da}{dN} = f(\Delta K) \Rightarrow \frac{\Delta a}{\Delta N_i} = f(\Delta K_i) \quad \Rightarrow \quad \Delta N_i = \frac{\Delta a}{f(\Delta K_i)} \tag{1}$$

4. The FE model is updated with the position of the new crack tip as shown in Figure 2. The area surrounding the crack tip may be remeshed if the user has activated this option.

Finally, the plug-in repeats Steps 2-4 with the new crack tip. For each iteration i, the plug-in records the total number of cycles $N_i = N_{i-1} + \Delta N_i$ and the current crack length $a_i = a_{i-1} + \Delta a$. The user can also request to save additional information such as the stress intensity factor range ΔK_i. This iterative procedure is repeated until (i) the number of iterations reaches a maximum value defined by the user or (ii) $\Delta N_i < 1$, meaning that crack growth has become unstable.

Loading the plug-in in Abaqus will open the GUI shown in Figure 3. This GUI includes four tabs where the user is prompted to enter all the information needed for the fatigue crack simulation. The subsections below will provide more information about each tab.

[1] Available at: https://doi.org/10.6084/m9.figshare.8038985.v1

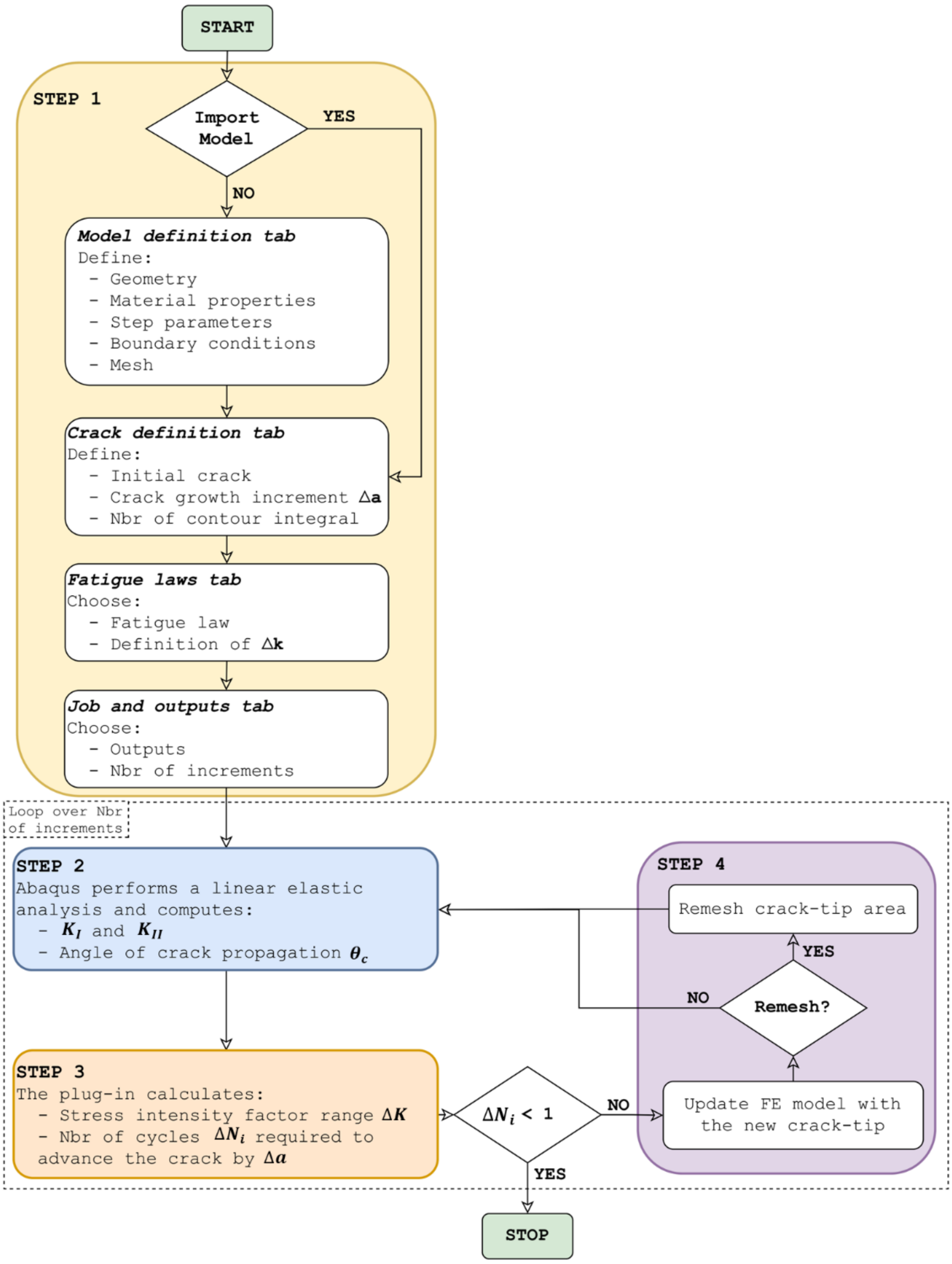

Figure 1. Flowchart of the plug-in to predict fatigue crack growth.

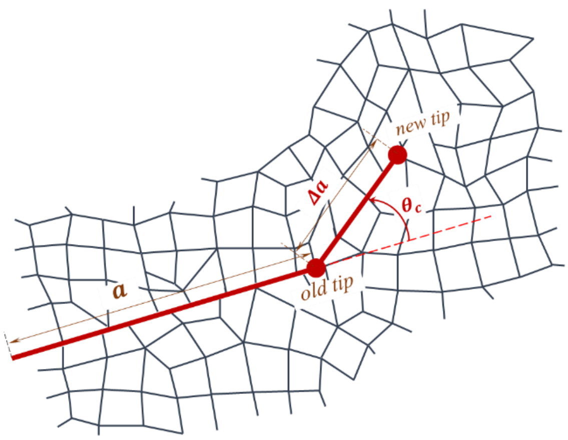

Figure 2. Representation of the fatigue crack growth increment Δa and the angle of crack propagation θ_c.

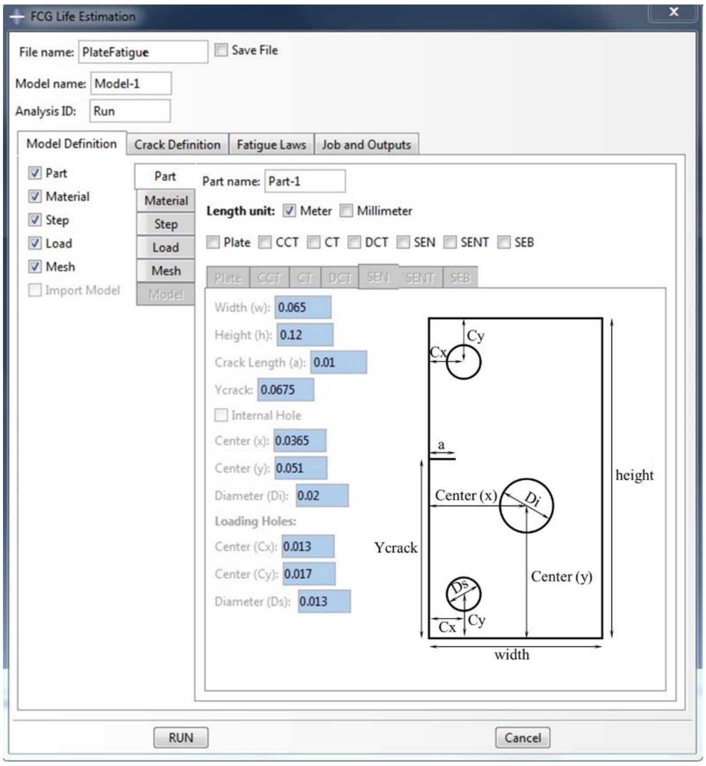

Figure 3. Main window of the plug-in.

2.1 *Model definition*

The first tab of the plug-in is *Model definition*, and this is where the user needs to define the geometry, material properties, step parameters, boundary conditions and mesh. All these parameters are specified in five submenus visible in Figure 3. The *Part* submenu allows the user to select one of six standard geometry specimens. These are shown in Figure 4 and include: center-cracked tension (CCT), compact tension (CT), disk-shaped CT (DCT), single-edge notched (SEN), single-edge notched under tension (SENT), and single-edge bending (SEB) specimens. These standard specimens are included to make it easier for new users to try the plug-in, and to compare numerical predictions with experimental data. Of course, users can also import their own geometry using the *Import model* submenu. More details about the import option are given at the end of this section.

Next, the user has to input the material properties using the *Material* submenu shown in Figure 5a. The material is modelled as linearly elastic and isotropic, characterized by its Young's modulus and Poisson's ratio. Moreover, since the geometry is 2D, the user has to specify the out-of-plane thickness of the geometry.

Recall that the plug-in uses Abaqus to perform a linear implicit simulation representing a single loading cycle (Step 2 in Figure 1). The *Step* submenu (Figure 5b) allows the user to specify the maximum number of iterations and the initial increment used during this calculation. Otherwise, the loading conditions are specified in the *Load* submenu shown in Figure 5c. Depending on the type of specimen selected, either the maximum pressure or point load can be specified. The minimum pressure or point load is specified using the load ratio R, defined as ratio of the minimum to the maximum force/pressure. Additionally, user can choose to apply a variable load and this option can be activated when needed, as shown in Figure 5c.

Finally, the *Mesh* submenu (Figure 5d) allows the user to define a fine element size to be used around the crack tip and a coarser one to be employed remotely. The user also has to choose between plane strain or plane stress elements. In addition, the plug-in offers possibility of remeshing around the updated crack-tip (Step 4 in Figure 1). Activating this option requires the user to define the new element size and area that will be re-meshed. This approach gives similar capabilities of the two-scale technique [19 , 20, 21] to only have very-fine mesh in a specific part of the problem. Note that the 2D implementation of XFEM in Abaqus uses four-node bilinear elements (in Abaqus notation these are CPS4 for plane stress and CPE4 for plane strain).

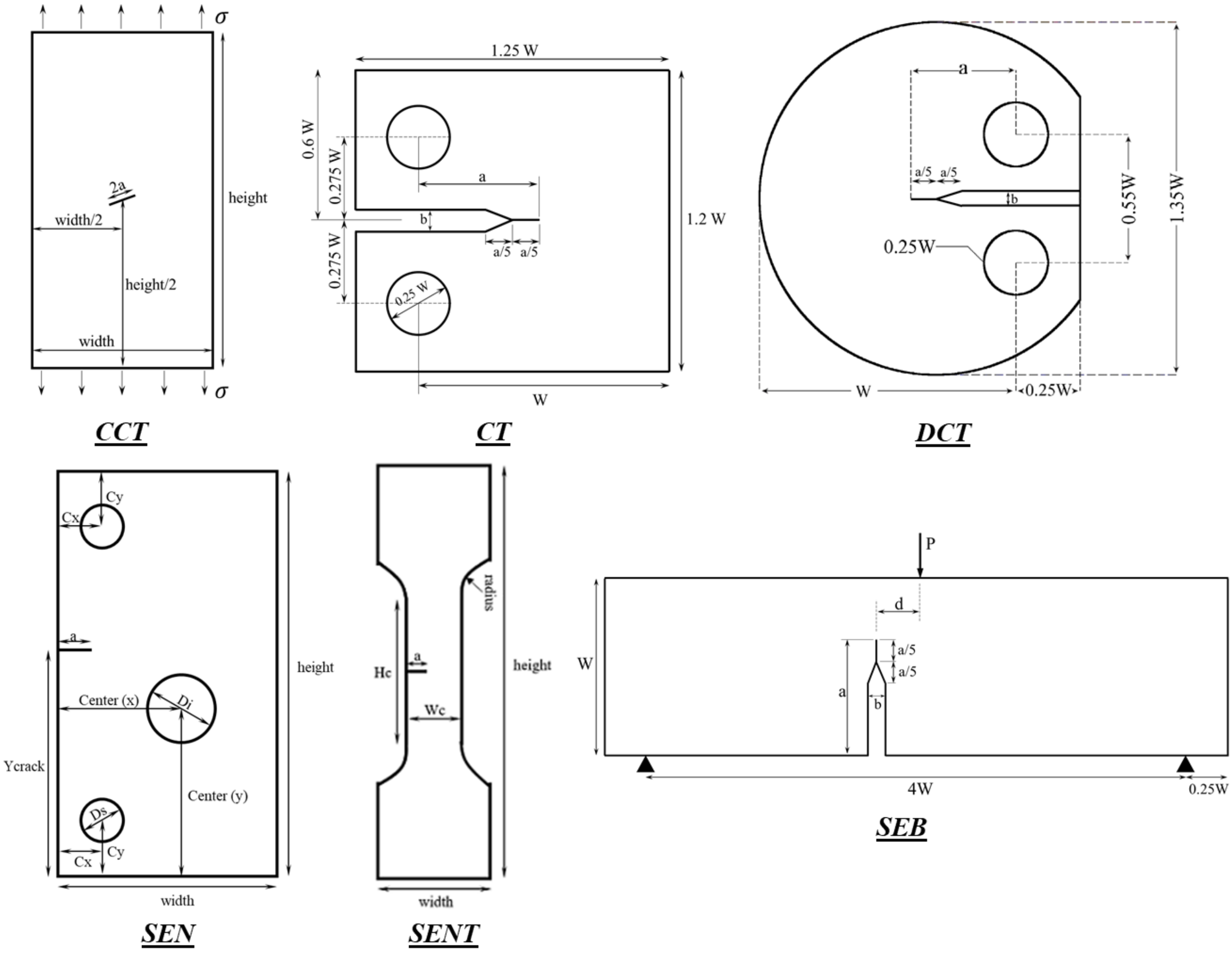

Figure 4. Standard specimens available in the plug-in.

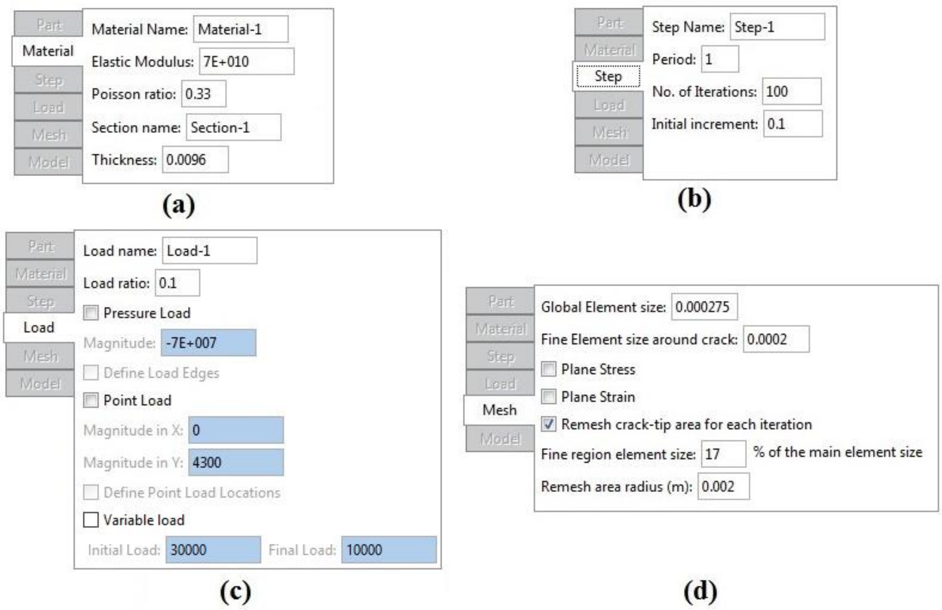

Figure 5. Definitions of: (a) material properties, (b) step parameters, (c) loading conditions, and (d) mesh.

As mentioned above, the user can import their own geometry instead of using one of the standard specimens shown in Figure 4. This is done using the *Import Model* checkbox and submenu as shown in Figure 6. The plug-in can import a model using either .cae or .inp files. Note that when this option is used, the model imported should include all elements mentioned above: the part, material properties, step parameters, mesh as well as boundary and loading conditions. Recall that this plug-in models crack propagation using XFEM; therefore, the imported geometry does not need to include an initial crack. Defining the initial crack is easily done with the plug-in, and this is described in the next subsection.

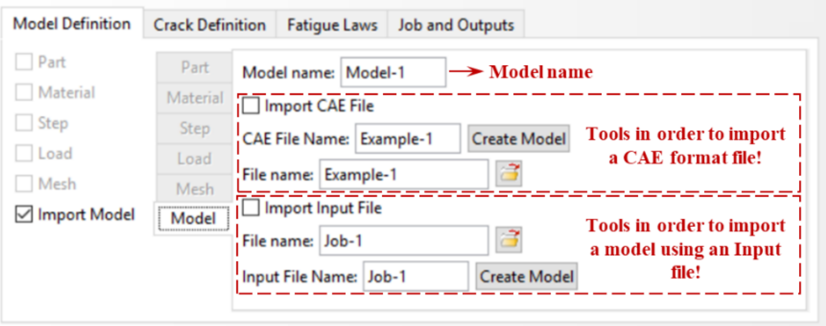

Figure 6. The import model option of the plug-in.

2.2 *Crack definition*

Once the geometry, mesh and loading conditions are defined, the next step is to define the initial crack using the *Crack definition* tab, see Figure 7. This plug-in does not support crack initiation and consequently the model requires an initial crack. Since this plug-in employs XFEM [22, 23], the initial crack is easily defined by entering its start and end coordinates. Another important input to specify in the *Crack geometry* submenu is the crack growth increment Δa. Recall that after each iteration, the crack will advance by Δa and the plug-in will compute how many cycles were needed for this growth (see Step 3 in Figure 1). Therefore, it is important that Δa is sufficiently small to ensure convergence of the results.

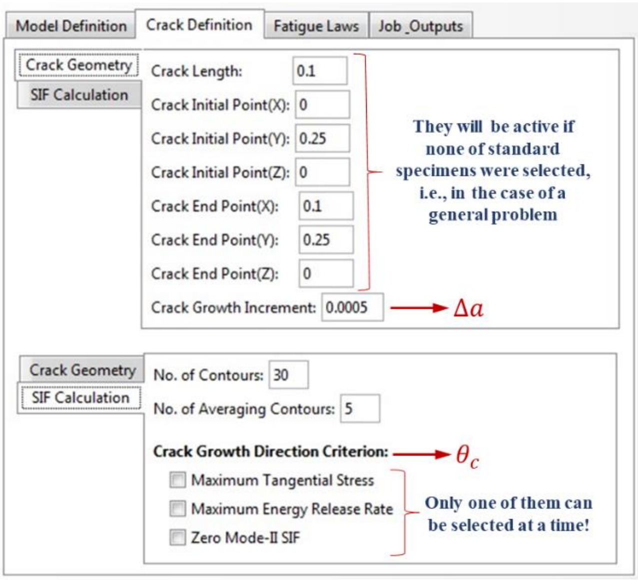

Figure 7. Crack definition and options to compute the stress intensity factors (re-organized for illustration only).

For each iteration, Abaqus will compute how the stress intensity factors K_I and K_{II} vary during a loading cycle. To achieve this, Abaqus first computes the *J*-integral and then uses an interaction integral method to extract K_I and K_{II} (consult the Abaqus documentation [24] for more details on this procedure). The plug-in asks the user to specify the number of contours that will be used to compute the *J*-integral, see Figure 7. The number of contours is roughly equal to the number of elements from the crack tip to the contour of the control domain as shown in Figure 8. The values of K_I and K_{II} computed by Abaqus can be mildly sensitive to the choice of contour; therefore, to alleviate this effect, the results can be averaged over a number of contours. For example, if the user sets the number of contours to 30 and the number of averaging contours to 5 then the values of K_I and K_{II} will be computed as the average for the 5 largest contours (26 to 30 inclusively).

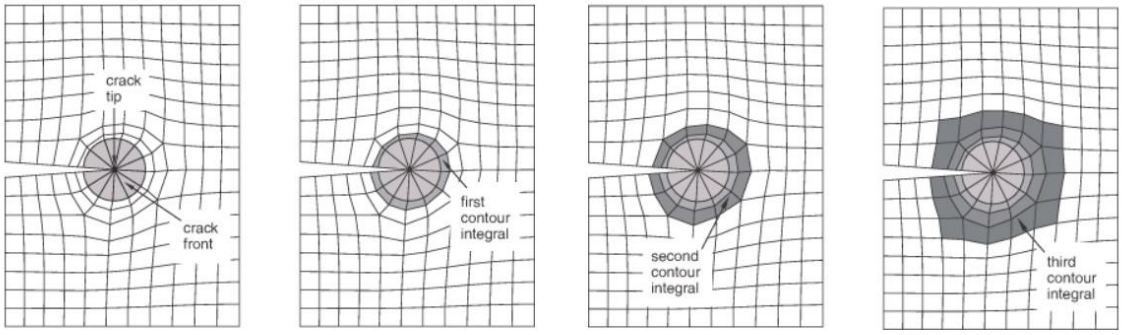

Figure 8. Schematic of the contour integral in Abaqus: successive contour integrals are calculated by adding a layer of elements. Adapted from [24].

Finally, the user is asked to select which criterion will be used to compute the direction of crack propagation θ_c (see Figure 2). Three options are available; the crack can follow the direction of (i) maximum tangential stress [25], or (ii) maximum energy release rate [25], or (iii) $K_{II} = 0$. These three criteria are included in Abaqus and therefore, the reader is referred to the Abaqus documentation [24] for more details. In short, the angle of crack propagation θ_c is calculated automatically by Abaqus at each iteration and using the maximum values of K_I and K_{II}, see Step 2 in Figure 1.

2.3 Fatigue laws

After defining the model and the initial crack, the user has to specify the fatigue crack growth parameters that will be used in the simulation. This is done via the *Fatigue law* tab, see Figure 9, where two elements need to be defined: (i) the approach to compute the stress intensity factor range ΔK and (ii) the fatigue crack growth model. These two aspects are reviewed below.

2.3.1 Calculation of the stress intensity factor range

During each iteration, Abaqus computes how the stress intensity factors K_I and K_{II} vary during a single loading cycle (see Step 2 in Figure 1). All fatigue crack growth models (see Section 2.3.2) are defined as a function of the stress intensity factor range ΔK, and therefore, we need to compute ΔK from the time histories of K_I and K_{II}. The plug-in offers five different ways of computing ΔK, and these are presented below.

First, ΔK_I and ΔK_{II} are defined as the difference between the maximum and minimum values (taken over a single loading cycle) of K_I and K_{II}, respectively. The simplest approach to define ΔK is to use:

$$\Delta K = \max(\Delta K_I\,;\Delta K_{II}) \tag{2}$$

Otherwise, an approach based on the energy release rate is to employ [26]:

$$\Delta K = \sqrt{\Delta K_I^2 + \Delta K_{II}^2} \tag{3}$$

where modes I and II have equal contributions. Tanaka [27] proposed another relationship where the two modes have different weightings. This is expressed as:

$$\Delta K = \sqrt[4]{\Delta K_I^4 + 8\Delta K_{II}^4} \tag{4}$$

Another expression for mixed-mode crack growth was proposed by Richard et al. [28]. They proposed to use:

$$\Delta K = \frac{\Delta K_I}{2} + \sqrt{\frac{\Delta K_I^2}{4} + \left(\frac{K_{Ic}}{K_{IIc}} \cdot \Delta K_{II}\right)^2} \tag{5}$$

where K_{Ic} and K_{IIc} are the fracture toughness for mode I and mode II, respectively. Finally, the fifth approach implemented in the plug-in is one developed by Tanaka et al. [29] and expressed as:

$$\Delta K = \Delta K_I \cos^3\left(\frac{\theta_c}{2}\right) - 3\Delta K_{II}\cos^2\left(\frac{\theta_c}{2}\right)\sin\left(\frac{\theta_c}{2}\right) \tag{6}$$

where θ_c is the angle of crack propagation introduced earlier and illustrated in Figure 2.

2.3.2 Fatigue crack growth models

The plug-in includes five fatigue crack growth models: Paris' law, Forman's law, Walker's law, NASGRO, and the approach of Erdogan and Ratwani [30]. In all cases, the crack growth rate da/dN is expressed as a function of the stress intensity factor range ΔK.

The most popular fatigue crack growth model is Paris' law, which can be expressed as [31, 32]:

$$\frac{da}{dN} = C(\Delta K - \Delta K_{th})^m \tag{7}$$

where C and m are material constants, and ΔK_{th} is the fatigue stress intensity threshold. A limitation of Paris' law is that it does not take into account the load ratio R. Forman et al. [33] proposed an alternative approach that includes the effect of the load ratio R. Forman's law is expressed as:

$$\frac{da}{dN} = \frac{C_f\, \Delta K^{m_f}}{(1-R)K_{Ic} - \Delta K} \tag{8}$$

where C_f and m_f are material constants, and K_{Ic} is the mode-I fracture toughness. Walker's law is also a modification of the Paris' law to include the load ratio R. Walker's law is expressed as [34]:

$$\frac{da}{dN} = C_w \left[\frac{\Delta K}{(1-R)^{1-\gamma}}\right]^{m_w} \tag{9}$$

where C_w, m_w and γ are material constants.

Paris', Forman's and Walker's laws all neglect the effect of the out-of-plane thickness on fatigue crack growth. However, reducing the thickness decreases the zone of high stress triaxiality inside the sample and this is known to influence the fracture toughness and fatigue crack growth [35]. Another fatigue crack growth model called NASGRO was developed to capture this dependency on thickness. This approach, which includes both the load ratio R and the out-of-plane thickness t, is written as [36]:

$$\frac{da}{dN} = \frac{C_n \left(\frac{1-f}{1-R}\Delta K\right)^n \left(1 - \frac{\Delta K_{th}}{\Delta K}\right)^p}{\left(1 - \frac{K_{max}}{K_{crit}}\right)^q} \tag{10}$$

where C_n, n, p and q are material constants; f is the Newman's function related to crack closure and its value can be found in [36]; and K_{crit} is the critical value of the stress intensity factor, which is dependent on the thickness t, and defined as:

$$\frac{K_{crit}}{K_{Ic}} = 1 + B_k e^{-(A_k t/t_0)^2} \tag{11}$$

where A_k and B_k are fitting constants, and the reference thickness $t_0 = 2.5(K_{Ic}/\sigma_y)^2$, where σ_y is the yield strength of the material. It is clear from Eq. (11) that K_{crit} tends to K_{Ic} when $t \gg t_0$.

The fourth model implemented in the plug-in is the approach developed by Erdogan and Ratwani [37]. They modified Forman's law to increase its accuracy when ΔK is close to ΔK_{th}. Their fatigue crack growth law is expressed as:

$$\frac{da}{dN} = \frac{C_e(1+\beta)^{q_e}\,(\Delta K - \Delta K_{th})^{p_e}}{K_{Ic}(1+\beta)\Delta K} \tag{12}$$

where C_e, p_e and q_e are material constants, and β is defined as:

$$\beta = \frac{1+R}{1-R} \tag{13}$$

We emphasize here that the approaches to compute ΔK are completely independent of the fatigue crack growth model. Therefore, any of the five approaches presented in Section 2.3.1 can be used with any of the five fatigue crack growth models presented above.

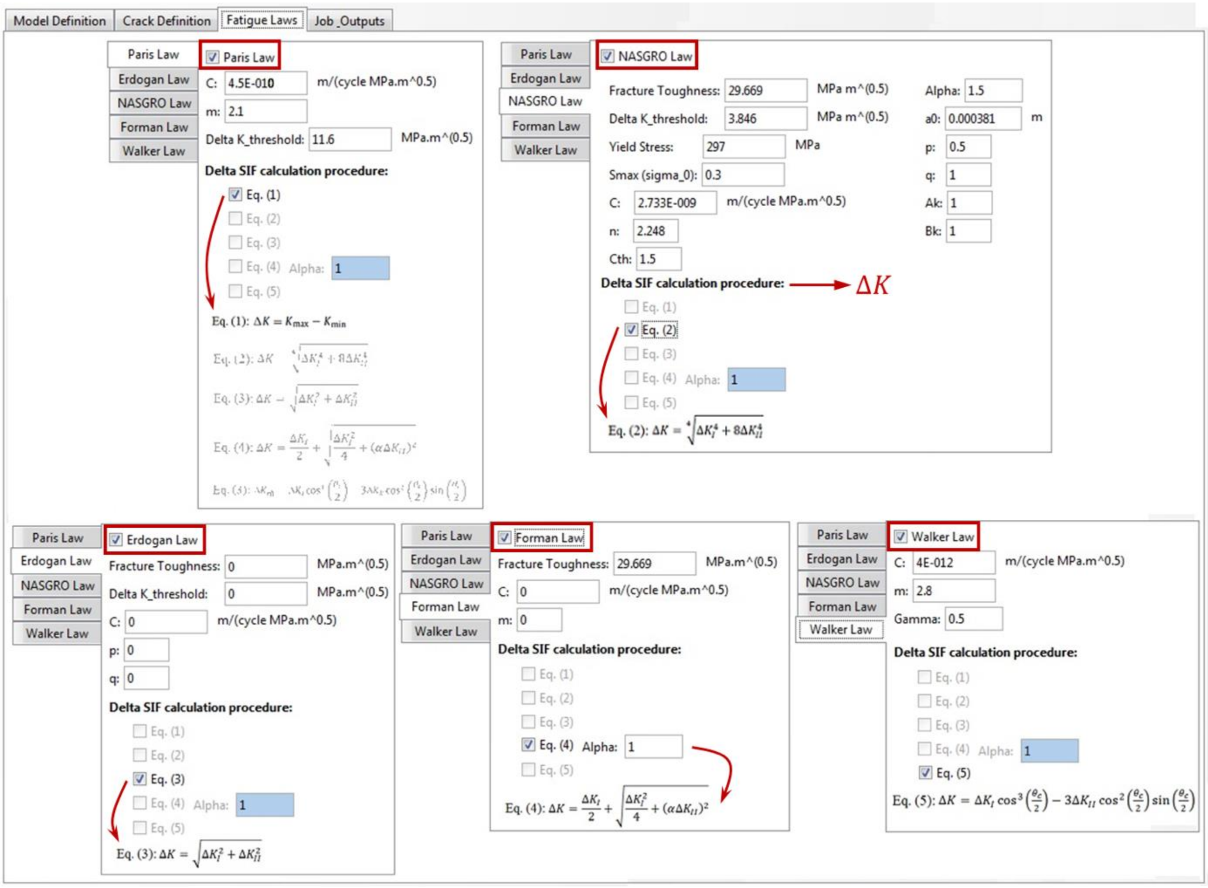

Figure 9. Fatigue law definition tab (re-organized for illustration only).

2.4 Job and outputs

The last step before running the fatigue crack growth simulation is to specify the desired output variables and a few parameters related to the job execution. These are entered in the *Job and Outputs* tab shown in Figure 10. In the submenu *Outputs*, the user can specify which variables should be recorded after each increment. These may include the coordinates of the crack tip (crack front); the angle of crack propagation θ_c; the minimum and maximum values of K_I and K_{II}; as well as ΔK_I , ΔK_{II} and ΔK. The user can request these variables to be plotted through the *Plots* submenu; the graphs can be generated as a function of the increment number or as a function of crack length. An example of the outputs and plots generated by the plug-in is given in Figure 11.

Recall that Abaqus performs a static simulation for each iteration of the plug-in (Step 2 in Figure 1). This procedure can generate a large number of files, which can be managed via the submenu *Output files*. There, the user can select which output files should be kept and their frequency.

Finally, the job execution parameters need to be entered in the *Job* submenu. This includes the job name, the number of processors to be used and the number increments for fatigue crack growth. Finally, one of four different checkbox needs to be activated:

- *Write Input File*: will generate the .inp file of the model without running the analysis.
- *Submit Job:* will run only steps 1 and 2 in Figure 1. This is useful to examine the stresses around the initial crack without simulating fatigue crack propagation.
- *Submit Incremental Job:* will lunch the complete fatigue crack growth simulation.
- *Write input data to a file:* will generate a text file containing all information entered in the plug-in windows.

Once all this information is provided, the analysis can be launched with the *run* button, see Figure 3.

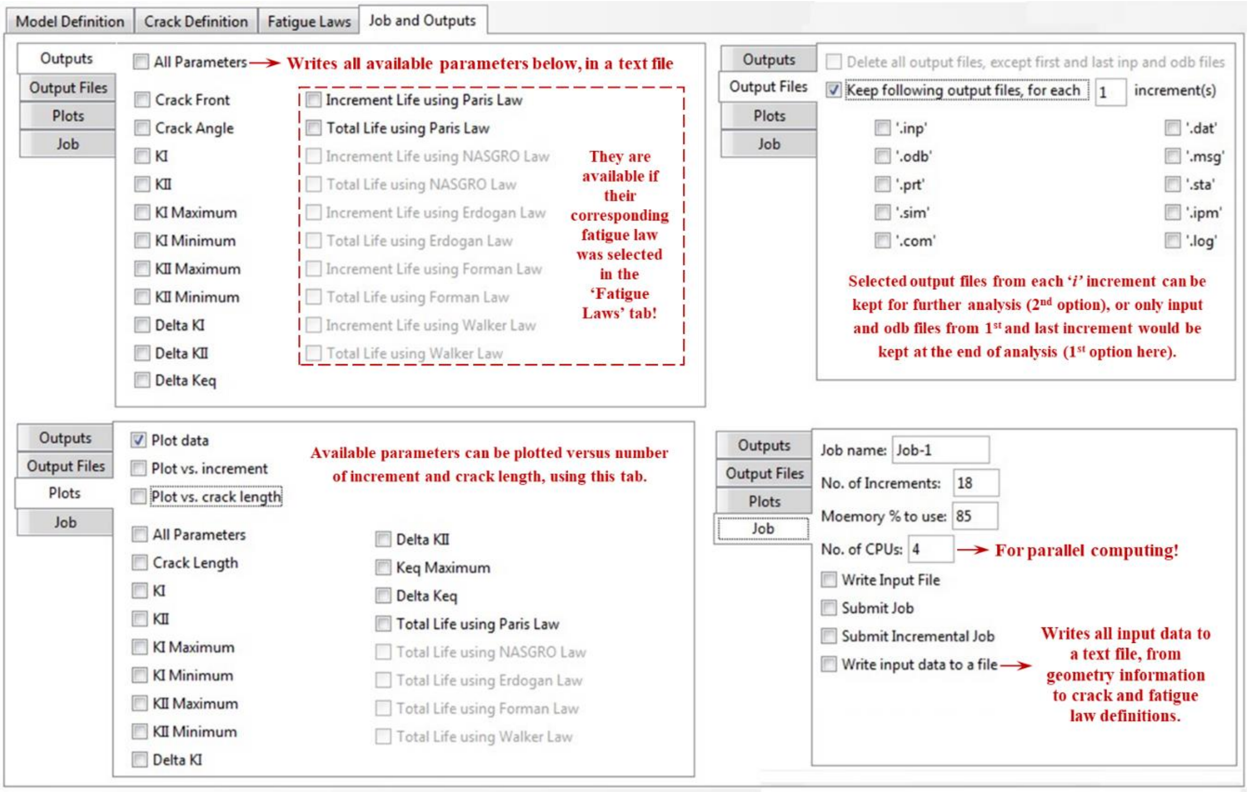

Figure 10. Output files and Job definition tab (re-organized for illustration only)

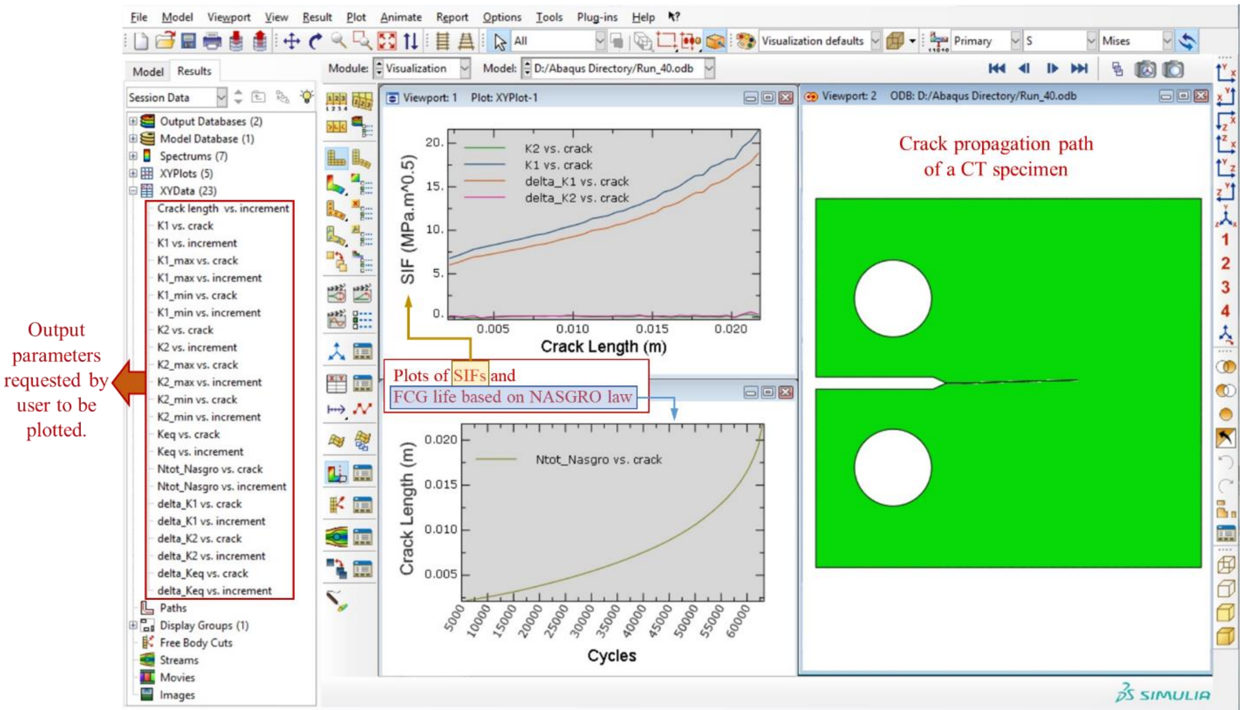

Figure 11. Visualization of the results in Abaqus/CAE.

3 Validation of the plug-in

In this section, simulation results are compared to analytical and experimental data to assess the accuracy of the plug-in. Three elements are considered in turn. Frist, the stress intensity factor computed by Abaqus is compared to analytical predictions. Second, predictions of crack length versus number of cycles are compared to experiments. Finally, predictions of the crack path are also compared to experimental data.

3.1 Calculation of the stress intensity factor

It is crucial that the plug-in computes accurately the stress intensity factors since all fatigue crack growth laws are expressed as a function of ΔK. As mentioned in Section 2.2, Abaqus first computes the J-integral and then uses an interaction integral method to calculate K_I and K_{II}. To ensure that this step is done accurately by the plug-in, we used a simple geometry to compare our numerical predictions to well-known analytical solutions.

For this comparison, we considered a CT specimen with dimensions shown in Figure 12a. The material had a Young's modulus $E = 160$ GPa and a Poisson's ratio $\nu = 0.28$; however, we emphasize that the material properties have no effect on the stress intensity factor. The load P applied to the specimen varied from 0 to 11 kN, creating pure mode-I conditions. A fine mesh size of 0.5 mm was used in the crack tip region and the sample had a total of 64,068 plane strain elements. The crack growth increment Δa was set to 0.5 mm, and no remeshing was done during the simulation. The choice of fatigue crack growth law is irrelevant for this example since we are interested only in K_I and K_{II}, not in the number of cycles N.

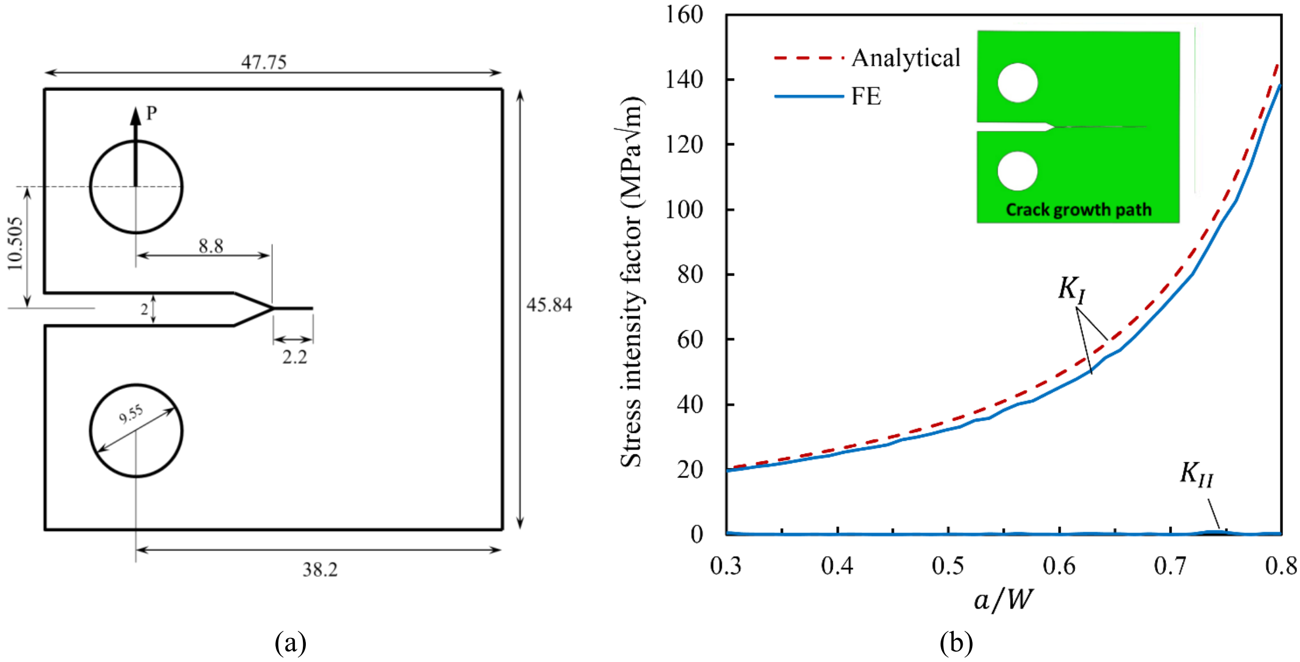

Figure 12. (a) Geometry of the CT specimen. All dimensions in mm. (b) Stress intensity factors as a function of the normalized crack length. Predictions from the plug-in (FE) are compared to analytical results. The crack growth path is included as an inset.

Numerical predictions for K_I and K_{II} are shown in Figure 12b as a function of the crack length a, which is normalized by the sample's width $W = 38.2$ mm. The analytical solution for K_I is also included in Figure 12b. According to ASTM [38], the mode I stress intensity factor for plane strain is given by:

$$K_I = \frac{P}{BW^{1/2}} \frac{2 + a/W}{(1 - a/W)^{3/2}} \left[0.866 + 4.64\left(\frac{a}{W}\right) - 13.32\left(\frac{a}{W}\right)^2 + 14.72\left(\frac{a}{W}\right)^3 - 5.6\left(\frac{a}{W}\right)^4\right] \quad (14)$$

where B is the thickness of the sample. The results in Figure 12a demonstrate that the stress intensity factor is calculated accurately throughout the simulation. Predictions for K_I are within 10% of the analytical values, and, as expected for a CT specimen, $K_{II} = 0$ throughout the simulation. The crack propagation path is also shown as an inset in Figure 12b: the crack grows in the initial crack plane and therefore, remains in a pure mode-I condition.

3.2 Fatigue life curves

In this section, we assess the accuracy of the plug-in to predict the crack length as a function of the number of cycles. For this comparison, we simulated the experiments done by Simunek et al. [39]. These fatigue tests were performed on steel S355 SENT specimens, and their dimensions are given in Figure 13a. The samples were tested with two different loading conditions: first, with a maximum tensile stress $\sigma = 100$ MPa and second, with $\sigma = 150$ MPa. In both cases, the load ratio $R = 0$.

These experiments were simulated using the same dimensions and loading conditions as those used during the tests. The steel was modelled with a Young's modulus $E = 200$ GPa and a Poisson's ratio $\nu = 0.3$. Paris' law was used to model fatigue crack growth using the following constants: $C = 4.5 \times 10^{-13}$ mm/cycle, $m = 3$, and $\Delta K_{th} = 6.6$ MPa√m. These values are within the range of measurements reported for this material in [39]. The mesh had a total of 37,975 plane strain elements, and the incremental crack growth Δa was set to 1 mm.

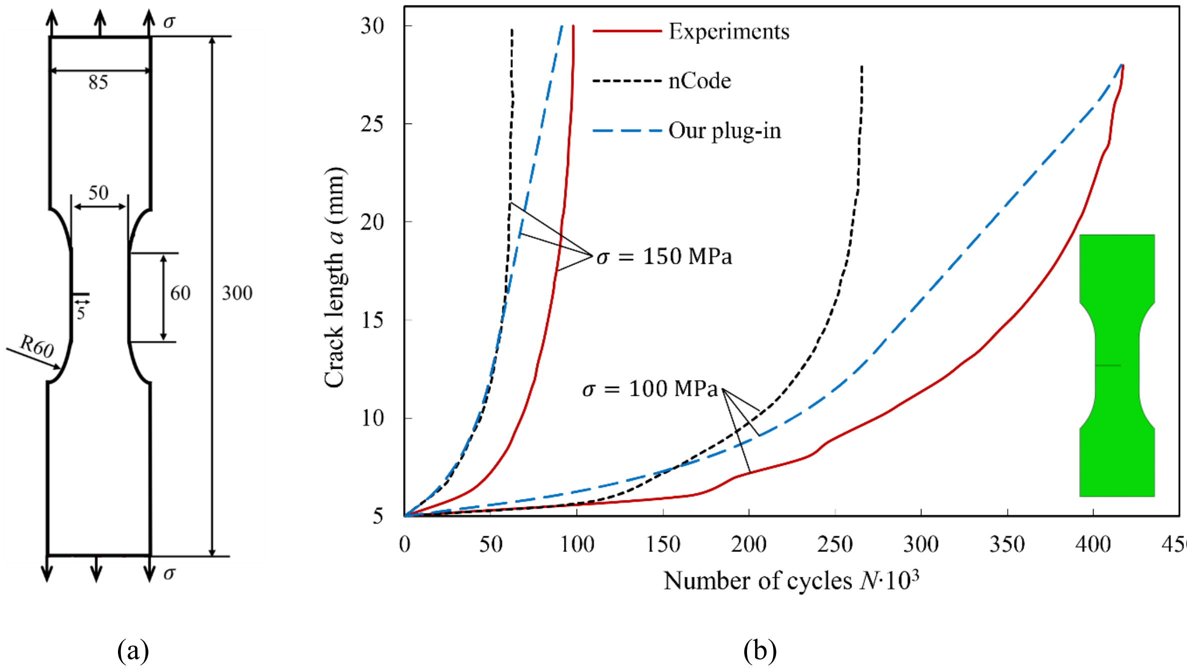

Figure 13. (a) Geometry of the SENT specimen. All dimensions in mm. (b) Fatigue life curves: our simulations are compared to experiments and predictions from Simunek et al. [39]. The crack growth path is included as an inset.

Our predictions are compared to experimental results in Figure 13b, where the crack length is plotted as a function of the number of cycles. Results are shown for both σ = 100 and 150 MPa. In addition, numerical predictions obtained by Simunek et al. [39] using the commercial software nCode are included for comparison. Note that these nCode simulations are also based on Paris' law, but the values of C, m and ΔK_{th} are not reported in [39].

Both sets of simulations (nCode and our plug-in) predict a faster crack growth than that observed in the experiments. Nonetheless, our predictions are more accurate than those obtained using nCode and show a reasonable agreement with experiments, especially for short crack lengths and when $\sigma = 100$ MPa. Note that for both $\sigma = 100$ and 150 MPa, the predicted crack path remains in the initial crack plane as shown in Figure 13b. This is in line with the experimental observations of Simunek et al. [39].

3.3 Crack path

Finally, we assessed the accuracy of the plug-in to predict the crack propagation path. Simulations were done for a SEN specimen of dimensions shown in Figure 14a. Four cases were considered where the initial crack was offset from the hole's center by a distance d_c = 16.5, 23, 30, and 36.6 mm. In all cases, a maximum force of 20 kN was used with a load ratio $R = 0.1$. The material had a Young's modulus $E = 71.7$ GPa and a Poisson's ratio $\nu = 0.33$; however, we emphasize that the material properties have a negligible effect on the crack path. The mesh had over 60,000 plane strain elements, and crack propagation followed the direction of maximum tangential stress.

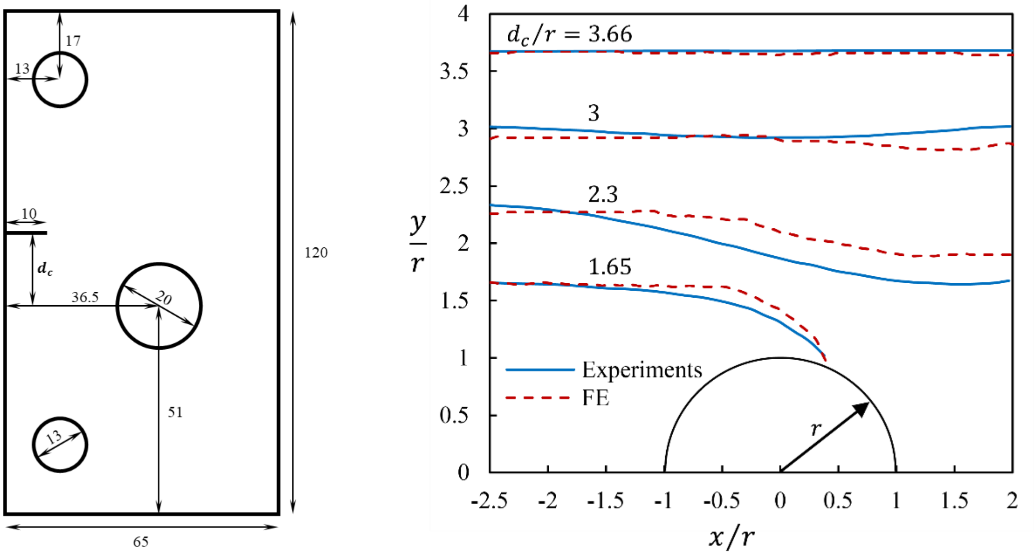

(a) (b)

Figure 14. (a) Geometry of the SEN specimen. All dimensions in mm. (b) The crack growth paths predicted by our plug-in are compared to experiments reported by Rubinstein [40].

The predicted crack paths are plotted in Figure 14b for four selected values of d_c. The FE simulations obtained with our plug-in are compared to experiments performed on similar geometries and reported by Rubinstein [40]. In all cases, the crack path predicted by the plug-in is in good agreement with experimental results.

4 Conclusion

An Abaqus plug-in was developed to simulate fatigue crack propagation. Even though it is limited to 2D analyses, the plug-in offers several advantages:

- The geometry of six standard specimens can be automatically generated, making it easier for new users to try the plug-in. Of course, users can also import their own geometry.
- Crack propagation is handled with XFEM, and the initial crack can be defined using coordinates only. This approach is simpler for the user since it does not require him/her to modify the part geometry to explicitly include the crack.
- The plug-in includes five fatigue crack growth laws, five ways of computing the stress intensity factor range for mixed-mode scenarios, and three criteria for the direction of crack propagation. This is significantly more choice than what is offered in many existing commercial tools.
- The plug-in will be freely distributed.

The accuracy of the plug-in was validated by comparing its predictions to analytical and experimental results taken from the literature. The plug-in was found to (i) accurately compute the stress intensity factors, (ii) simulate crack growth curves with reasonable accuracy, and (iii) accurately predict the crack path for mixed-mode loading scenarios.

We believe that this plug-in can be a useful tool to simulate crack propagation, especially for educational and research activities. Future work is underway to extend the plug-in to incorporate multiple cracks, and to expand its formulation to 3D problems, and including the crack closure effects in the FCG life estimation process. Another interesting topic to include in the future version of this plug-in is the capability to model micro-voids/inclusions interacting with the main fatigue crack, similar to those presented in [11, 41].

References

[1] Lesiuk G, Smolnicki M, Rozumek D, Krechkovska H, Student O, Correia J, Mech R, de Jesus A (2020) Study of the fatigue crack growth in long-term operated mild steel under mixed-mode (I + II, I + III) loading conditions. *Materials* 13(1):160. doi: 10.3390/ma13010160

[2] Silva ALL, Correia JAFO, de Jesus AMP, Lesiuk G, Fernandes AA, Calçad R, Berto F (2019) Influence of fillet end geometry on fatigue behaviour of welded joints. *Int. J. Fatigue* 123:196-212. doi: 10.1016/j.ijfatigue.2019.02.025

[3] Rozumek D, Marciniak Z, Lesiuk G, Correia JA, de Jesus AMP (2018) Experimental and numerical investigation of mixed mode I+II and I+III fatigue crack growth in S355J0 steel. *Int. J. Fatigue* 113:160-170. doi: 10.1016/j.ijfatigue.2018.04.005

[4] Paris P, Erdogan F (1963) A critical analysis of crack propagation laws. *Trans. ASME* 85 (4):528-533. doi: 10.1115/1.3656900

[5] Forman RG, Kearney VE, Engle RM (1967) Numerical analysis of crack propagation in cyclic-loaded structures. *J. Basic Eng.* 89(3):459-463. doi: 10.1115/1.3609637

[6] Schütz W (1996) A history of fatigue. *Eng. Fract. Mech.* 54(2):263-300. doi: 10.1016/0013-7944(95)00178-6

[7] Correia JAFO, Blasón S, Arcari A, Calvente M, Apetre N, Moreira PMGP, de Jesus AMP, Canteli AF (2016) Modified CCS fatigue crack growth model for the AA2019-T851 based on plasticity-induced crack-closure. *Theo. Applied Fract. Mech.* 85:26-36. doi: 10.1016/j.tafmec.2016.08.024

[8] Correia JAFO, de Jesus AMP, Moreira PMGP, Tavares PJS (2016) Crack closure effects on fatigue crack propagation rates: application of a proposed theoretical model. *Adv. Mater. Sci. Eng.* 3026745. doi: 10.1155/2016/3026745

[9] Duan QY, Li JQ, Li YY, Yin YJ, Xie HM, He W (2020) A novel parameter to evaluate fatigue crack closure: Crack opening ratio. *Int. J. Fatigue* 141:105859. doi: 10.1016/j.ijfatigue.2020.105859

[10] Silva ALL, de Jesus AMP, Xavier J, Correia JAFO, Fernandes AA (2017) Combined analytical-numerical methodologies for the evaluation of mixed-mode (I + II) fatigue crack growth rates in structural steels. *Eng. Fract. Mech.* 185:124-138. doi:

[11] Malekan M, Carvalho H (2018) Analysis of a main fatigue crack interaction with multiple micro-cracks/voids in a compact tension specimen repaired by stop-hole technique. *J. Strain Anal. Eng.* 53(8):648-662. doi: 10.1177/0123456789123456

[12] Nesládek M, Španiel M (2017) An Abaqus plugin for fatigue predictions. *Adv. Eng. Softw.* 103:1–11. doi: 10.1016/j.advengsoft.2016.10.008

[13] ZENCRACK manual, Version 7.9.

[14] http://gem-innovation.com/project/xfa3d/

[15] Lani F, Wyart E, Laurent D (2013) A XFEM-based probabilistic damage tolerant approach with Morfeo/Crack for Abaqus.Simulia Benelux Users' Meeting (Conferentiecentrum Bovendonk – Hoeven, Netherlands, du 13/11/2013 au 14/11/2013)

[16] He W, Liu J, Xie D (2014) Numerical study on fatigue crack growth at a web-stiffener of ship structural details by an objected-oriented approach in conjunction with ABAQUS. *Marine Struct.* 35:45–69. doi: 10.1016/j.marstruc.2013.12.001

[17] Pedersen MM (2016) Multiaxial fatigue assessment of welded joints using the notch stress approach. *Int. J. Fatigue* 83(2):269-279. doi: 10.1016/j.ijfatigue.2015.10.021

[18] Malekan M, Khosravi A, St-Pierre L. (2019) An Abaqus plug-in to simulate fatigue crack growth - Supporting materials. figshare. Software.

[19] Noor AK (1986) Global-local methodologies and their application to nonlinear analysis. *Finite Elem. Anal. Des.* 2:333-346. doi: 10.1016/0168-874X(86)90020-X

[20] Malekan M, Barros FB (2016) Well-conditioning global–local analysis using stable generalized/extended finite element method for linear elastic fracture mechanics. *Comput. Mech.* 58(5):819-831. doi: 10.1007/s00466-016-1318-7

[21] Malekan M, Barros F, Pitangueira RLS (2018) Fracture analysis in plane structures with the two-scale G/XFEM method. *Int. J. Solids Struct.* 155:65-80. doi: 10.1016/j.ijsolstr.2018.07.009

[22] Belytschko T, Black T (1999) Elastic crack growth in finite elements with minimal remeshing. *Int. J. Numer. Methods Eng.* 45:601-620. doi: 10.1002/(SICI)1097-0207(19990620)45:5<601::AID-NME598>3.0.CO;2-S

[23] Strouboulis T, Copps K, Babuska I (2000) The generalized finite element method: an example of its implementation and illustration of its performance. *Int. J. Numer. Methods Eng.* 47:1401-1417. doi: 10.1002/(SICI)1097-0207(20000320)47:8<1401::AID-NME835>3.0.CO;2-8

[24] Dassault Systémes Simulia Corp., Abaqus user's manual, version 6.14-2, Providence, Rhode Island, USA, 2014.

[25] Erdogan F, Shi GC (1963) On the crack extension in plates under plane loading and transverse shear. *J. Basic Eng.* 85(4):519-525. doi:10.1115/1.3656897

[26] Pais MJ (2011) Variable amplitude fatigue analysis using surrogate models and exact XFEM reanalysis. PhD thesis, University of Florida, USA.

[27] Tanaka K (1974) Fatigue crack propagation from a crack inclined to the cyclic tension axis. *Engrg. Fract. Mech.* 6:493–507. doi: 10.1016/0013-7944(74)90007-1

[28] Richard HA, Buchholz FG, Kulmer G, Schollmann M (2003) 2D and 3D mixed mode criteria. *Adv. Fract. Damage Mech.* 251:251–260. doi: 10.4028/www.scientific.net/KEM.251-252.251

[29] Tanaka K, Akiniwa Y, Kato T, Takahashi H (2005) Prediction of fatigue crack propagation path from a pre-crack under combined torsional and axial loading. *Jpn. Soc. Mech. Eng.* 71(703):607-614[in Japanese]. doi: 10.1299/kikaia.71.607

[30] Erdogan F, Ratwani M (1970) Fatigue and fracture of cylindrical shells containing circumferential cracks. *Int. J. Fract. Mech.* 6(4):379-392. doi: 10.1007/BF00182626

[31] Paris PC, Gomez M, Anderson W (1961) A Rational Analytic Theory of Fatigue. *Trend in Eng.* 9-14.

[32] Paris PC (1963) A critical analysis of crack propagation laws. *J. Basic Eng.* 85:528–534.

[33] Forman RG, Kearney VE, Engle RM (1967) Numerical analysis of crack propagation in cyclic loaded structures. *J. Basic Eng.* 89(3):459-463.

[34] Walker K (1970) The effect of stress ratio during crack propagation and fatigue for 2024-T3 and 7075-T6 Aluminum. In Effects of Environment and Complex Load History for Fatigue Life, Special Technical Publication 462, pp. 1-14. Philadelphia: American Society for Testing and Materials.

[35] Anderson TL (2005) *Fracture Mechanics: Fundamentals and Applications*. Third Edition, CRC press.

[36] AFGROW. Fracture mechanics and fatigue crack growth analysis software tool. V. 4.12.15.0, LexTech Inc., USA.

[37] Erdogan F, Ratwani M (1970) Fatigue and fracture of cylindrical shells containing circumferential cracks. *Int. J. Fract. Mech.* 6(4):379-392. doi: 10.1007/BF00182626

[38] ASTM (2015) ASTM International, 2015. ASTM E647 - 15 Standard test method for measurement of fatigue crack growth rates. In United States: ASTM International, p. 43. Available at: http://www.astm.org/Standards/E647.

[39] Simunek D, Leitner M, Maierhofer J, Gänser H-P (2015) Fatigue crack growth under constant and variable amplitude loading at semi-elliptical and V-notched steel specimens. *Proc. Eng.* 133:348 – 361. doi: 10.1016/j.proeng.2015.12.670

[40] Rubinstein AA (1991) Mechanics of the crack path formation. *Int. J. Fract.* 41:29 l-305. doi: 10.1007/BF00012948

[41] Malekan M, Barros FB (2018) Numerical analysis of a main crack interactions with micro-defects/inhomogeneities using two-scale generalized/extended finite element method. *Comput. Mech.* 62(4):783-801. doi: 10.1007/s00466-017-1527-8